Wave front equation, caustics, and wave aberration function of simple lenses and mirrors

Abd M. Kassim and David L. Shealy

Using the condition of constant optical path length for rays passing through an optical system, an equation for the wave front is presented in a simplified form. The wave front equation has been explicitly evaluated for a plane wave incident on a spherical reflector or a plano-convex lens. Then, the principal radii of curvature of the reflected or refracted wave front, evaluated directly from the wave front equation, are shown to locate the caustic surfaces of the optical system. From the wave front equation, a closed form expression for the wave aberration function for a plane wave reflected by a spherical mirror or a plano-corvex lens has been evaluated and compared to the results obtained from third-order aberration theory.

I. Introduction

The high degree of nonlinearity of the equations of geometrical optics does not permit an analytical derivation of a closed form expression for the wave front reflected or refracted by a general optical system. Based on the Fresnel formulas[1] and Hamiltonian optics,[2] Fock[3] derived an expression for a spherical wave front reflected from one surface with an arbitrary shape. Fock evaluates the wave front curvatures which are used to study the energy flux density behavior after reflection. Stavroudis and Fronczek[4] derived an expression for the wave front by integrating the eikonal equation. Stavroudis[5] also presented a set of differential equations whose solution represents the wave front after refraction of light from a point source by a spherical surface. Kneisly[6] derived equations that connect the local curvatures of the emerging wave front of the incident wave front and of the deflecting surface. These equations have been integrated by Rebordao and Grossmann[7] to yield a parametric description of the train of the refracted wave fronts by a single spherical surface. The deviation of the wave front from a spherical shape is, in general, caused by aberrations of the system.

An analysis of the aberrations in geometrical optics (ray and wave aberrations) has been carried out by Seidel,[8] who took into account all the terms of the third order in a general centered system of spherical surfaces. Subsequently, Buchdahl[9] has extended Seidel's work to higher orders. Sands[10] developed a method for evaluating the off-axis aberration coefficients. His method of derivation is similar to that of Buchdahl with pseudoexpansions and iterations being used. Using the optical path length as an invariant, Welford[11] derived an expression for computing the total wave aberration function. Hopkins[12] introduced an entirely different approach for calculating the wave front aberration function by defining invariant foci for which the optical aberrations remain constant as the wave front propagates through the system.

In this paper, an equation for the wave front surface passing through an optical system is given as a function of the entrance pupil coordinates and the optical path length obtained from geometrical optics.[13] For on- and off-axis incidence of light on a spherical reflector, an analytical expression for the reflected wave front surface has been derived. Using results from differential geometry,[14] the principal radii of curvature of the reflected wave front have been evaluated. A similar study has been carried out for the wave front refracted by a plano-convex lens. These expressions for the principal radii of curvature of the reflected (or refracted) wave front surface have been shown to locate the caustic surfaces of the system.[15,16] The comparison establishes that the caustic surface represents the loci of the singularities in the flux density as well as the loci of the centers of curvature of the emergent wave front surface.[16] Also presented in this paper is an analytical expression for wave aberration function of these systems.[17] For on-axis incidence on a spherical reflector and a plano-convex lens, the wave aberration function has been evaluated and compared to the corresponding

The authors are with University of Alabama in Birmingham, Physics Department, Birmingham, Alabama 35294.

Received 28 May 1987.
0003-6935/88/030516-07$02.00/0.

values given by third- and fifth-order aberration theory.[18]

II. Wave Front Equation

Using finite ray tracing and the condition of constant optical path length for all rays passing through an optical system, the emergent wave front surface can be evaluated as it passes through the center of the exit pupil. Referring to Fig. 1, consider a ray intercept with the last optical surface to be given by $\mathbf{X}_N$. Then a point on the emergent wave front surface is given by

$$\mathbf{X}_W = \mathbf{X}_N + \delta(x_p,y_p,\alpha)\hat{A}_N, \tag{1}$$

where the parameter δ measures the distance along the ray from $\mathbf{X}_N$ to the wave front surface, the coordinates (x_p,y_p) specify the entrance pupil coordinates, and α is the angle which the incident ray makes with the optical axis. The unit vector $\hat{A}_N$ along the emerging ray from the optical interface S_N can be evaluated using the vector form of Snell's law[19]:

$$\mathbf{A}_N = \gamma_N\hat{A}_{N-1} + (-\gamma_N \cos\theta_N + \cos\theta_N')\hat{N}_N, \tag{2}$$

where for reflection $\gamma_N = -1$ and for refraction $\gamma_N = n_{N-1}/n_N$. $\hat{N}_N$ is a unit vector normal to the optical interface surface S_N at the point of incidence and has the same general orientation as $\hat{A}_N$. The quantities θ_N and θ_N' are the angles of incidence and refraction.

Since points on the wave front surface are the same optical distance from the object point, a constraint equation for the wave front surface at different points within the optical system is given by

$$n_N\delta(x_p,y_p\alpha) + \psi(x_p,y_p,\alpha) = \psi_0, \tag{3}$$

where ψ_0 is a constant which is equal to the optical path length of the principal ray[20] from the incident wave front surface at the entrance pupil to the center of the exit pupil, which is considered to be a plane located at the vertex of the last optical surface normal to the optical axis. The quantity $\psi(x_p,y_p,\alpha)$ is equal to the optical path length of an arbitrary ray measured from the incident wave front surface (a plane since the source is at infinity) at a particular time when the principal ray intercepts the optical axis at the entrance pupil to the point where this arbitrary ray leaves the last optical surface (see Fig. 1). For multiple interface media whose indices of refraction are not a function of position in the individual media, ψ is given by

$$\psi(x_p,y_p;\alpha) = \sum_{N-1}^{k=0} n_k r_k(x_p,y_p;\alpha), \tag{4}$$

where n_k is the refractive index of the media to the right of the S_k surface, and r_k is the distance along the ray passing from the S_k to S_{k+1} surface. The surface S_0 is the surface of the incident wave front as the principal ray intercepts the optical axis at the entrance pupil. Referring to Eq. (4), the position of the wave front surface propagating through the optical system can be located by a particular choice of the parameter ψ_0 which is chosen so that the emergent wave front surface is located at the center of the exit pupil E.

Combining Eqs. (1), (3), and (4) gives

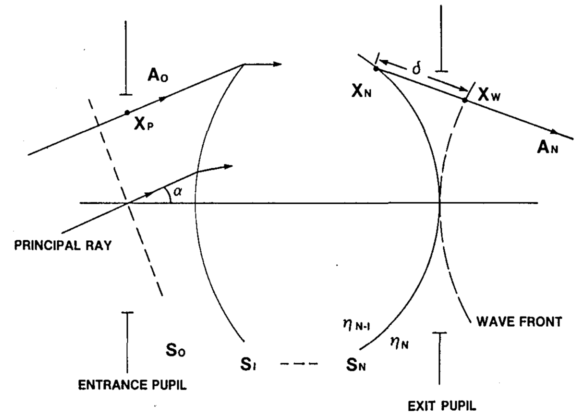

Fig. 1. Refracted wave front configuration for a general optical system.

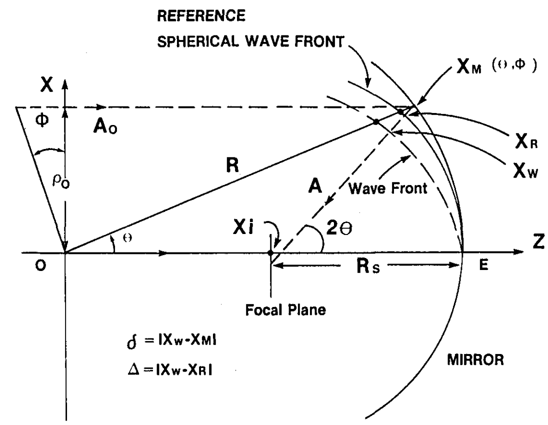

Fig. 2. On-axis reflection of plane wave by a spherical reflector.

$$\mathbf{X}_w = \mathbf{X}_N + \left[\psi_0 - \sum_{k=0}^{N-1} n_k r_k(x_p,y_p;\alpha)\right]\hat{A}_N/n_N. \tag{5}$$

Equation (5) will now be specialized to plane wave reflection or refraction from a spherical mirror and plano-convex lens and will be used to evaluate the emergent wave front principal radii of curvature and wave aberration function.

III. Wave Front Principal Curvatures

For the case of plane wave reflection from spherical mirror or refraction from a plano-convex lens, Eq. (5) can be written in a closed form. Then the formulas for emerging wave front principal curvatures can be expressed in a closed form, using results from differential geometry.[14]

A. Spherical Reflector

Consider an axial ray incident on a spherical reflector of radius R, where the mirror center is located at the origin of the coordinate system (see Fig. 2). Then the unit vector along the reflected ray $\hat{A}$ can be expressed as[15]

$$\hat{A}(\theta,\phi) = -\cos\phi \sin 2\theta\hat{i} - \sin\phi \sin 2\theta\hat{j} - \cos 2\theta\hat{k}, \tag{6}$$

where (θ,ϕ) are spherical coordinates of the reflection point on the mirror. The position vector of the incident point on the spherical reflector is given by

$$\mathbf{X}_m(\theta,\phi) = R\sin\theta\cos\theta\hat{i} + R\sin\theta\sin\phi j + R\cos\phi\hat{k}. \tag{7}$$

Since the object is at infinity, one needs a reference plane so that all rays have the same phase as they pass through that plane. For simplicity, this plane, which is called the entrance pupil, is the xy plane located at the origin of the coordinate system (see Fig. 2). Then the principal ray is along the optical axis (z axis). The center of the exit pupil is considered as the vertex of the spherical reflector E. For the on-axis incidence from air on a spherical reflector, $\psi_0 = R$ and $\psi = R\cos\theta$. Then Eq. (5) can be written as

$$\mathbf{X}_w(\theta,\phi) = R[\sin\theta - (1-\cos\theta)\sin 2\theta](\cos\theta\hat{i} + \sin\phi\hat{j}) + R[\cos\theta - (1-\cos\theta)\cos 2\theta]\hat{k}. \tag{8}$$

Equation (8) represents the vector position of the reflected wave front surface as it passes through the exit pupil. This equation will be used to derive expressions for the principal radii of curvature of the refracted wave front surface.

The first fundamental quantities of the reflected wave front are computed as follows[14]:

$$g_{\theta\theta} = \frac{\partial \mathbf{X}_w}{\partial\theta}\cdot\frac{\partial \mathbf{X}_w}{\partial\theta} = R^2(3\cos\theta - 2)^2; \tag{9a}$$

$$g_{\phi\phi} = \frac{\partial \mathbf{X}_w}{\partial\theta}\cdot\frac{\partial \mathbf{X}_w}{\partial\theta} = R^2[\sin\theta - \sin 2\theta(1-\cos\theta)]; \tag{9b}$$

$$g_{\theta\phi} = \frac{\partial \mathbf{X}_w}{\partial\theta}\cdot\frac{\partial \mathbf{X}_w}{\partial\theta} = 0. \tag{9c}$$

The second fundamental quantities of the reflected wave front are given by[14]

$$b_{\theta\theta} = \hat{A}\cdot\frac{\partial^2 \mathbf{X}_w}{\partial\theta^2} = 2R(3\cos\theta - 2), \tag{10a}$$

$$b_{\phi\phi} = \hat{A}\cdot\frac{\partial^2 \mathbf{X}_w}{\partial\theta^2} = R\sin\theta\sin 2\theta(1 - 2\cos\theta + 2\cos^2\theta), \tag{10b}$$

$$b_{\theta\phi} = \hat{A}\cdot\frac{\partial^2 \mathbf{X}_w}{\partial\theta\partial\phi} = 0. \tag{10c}$$

Since $g_{\theta b} = 0 = b_{\theta b}$, the curves on the wave front surface θ = constant and ϕ = constant are along the principal directions.[21] The principal curvatures of the reflected wave front surface, K_θ, and K_ϕ, are expressed by

$$K_\theta = \frac{b_{\theta\theta}}{g_{\theta\theta}} = \frac{2}{R(3\cos\theta - 2)}, \tag{11a}$$

$$K_\phi = \frac{b_{\phi\phi}}{g_{\phi\phi}} = 2\cos\theta/[R(1 - 2\cos\theta + 2\cos^2\theta)]. \tag{11b}$$

The values of K_θ and K_ϕ are graphed as a function of the normalized entrance pupil radius (ρ_0/R) in Fig. 3. The values of K_θ and K_ϕ are similar for small values of ρ_0, i.e., paraxial incidence, while the tangential curvature K_θ increases more rapidly than the corresponding sagittal curvature K_ϕ for large entrance pupil radii. This means the image will be more spread out in the tangential direction due to the spherical aberration[22] than in the sagittal direction.

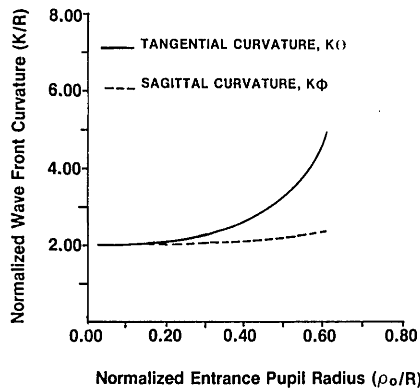

Fig. 3. Principal curvatures of the reflected wave front as a function of the entrance pupil radius for on-axis incidence on a spherical reflector.

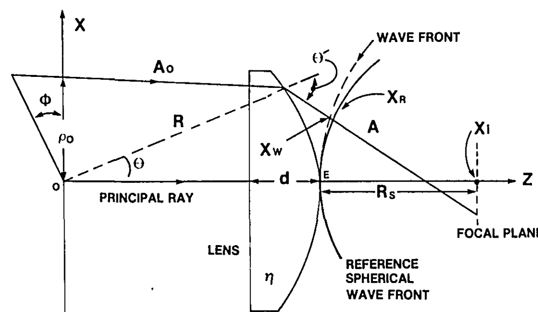

Fig. 4. On-axis refraction of plane wave by a plano-convex lens.

For the axial incidence on the optical axis (θ = 0), Eqs. (11a) and (11b) reduce to

$$K_\theta = K_\phi = -2/R. \tag{12}$$

Equation (12) establishes that the reflected wave front at the center of the exit pupil has two identical principal radii of curvature (no aberrations), and the center of curvature of that wave front is located at the ideal image point.[23]

B. Plano-Convex Lens

Equation (5) will be simplified for the case of refraction of an axial incident plane wave on a plano-convex lens. Consider a collimated axial ray incident on a plano-convex lens shown in Fig. 4. The unit vector along the refracted emerging ray $\hat{A}$, can be expressed by using Snell's law, Eq. (2), to give

$$\hat{A}(\theta,\phi) = -\cos\theta\sin(\phi'-\theta)\hat{i} - \sin\phi\sin(\phi'-\theta)j + \cos(\phi'-\theta)\hat{k}. \tag{13}$$

Since the direction of the principal ray is taken along the optical axis (z axis), ψ_0 and ψ are given by (see Fig. 4)

$$\psi_0 = R + (n-1)d, \quad (14a)$$

$$\psi = R + (n-1)d - nR(1-\cos\theta), \quad (14b)$$

where d is the lens thickness. Combining Eqs. (5), (7), (13), (14a), and (14b) gives

$$\mathbf{X}_w(\theta,\phi) = R[\sin\theta - n(1-\cos\theta)\sin(\phi'-\theta)][\cos\theta\hat{i} + \sin\phi\hat{j}] + R[\cos\theta + n(1-\cos\theta)\cos(\theta'-\theta)]\hat{k}. \quad (15)$$

Equation (15) represents an analytical expression for the refracted wave front surface as it propagates through the exit pupil. Using the results of the differential geometry,[14] one can evaluate the principal radii of curvature of the refracted wave front surface for Eq. (15). The first fundamental quantities are expressed as

$$g_{\theta\theta} = R^2[\cos\theta' + n(\cos\theta' - 1)/\cos\theta], \quad (16a)$$

$$g_{\phi\phi} = R^2[\sin\theta - n(1-\cos\theta)\sin(\phi'-\theta)]^2, \quad (16b)$$

$$g_{\theta\phi} = 0. \quad (16c)$$

The second fundamental quantities are given by

$$b_{\theta\theta} = \frac{\sec\theta}{R}[n\sec^2\theta - \cos(\theta'-\theta) \times \sec^2\theta\left(\frac{n\cos\theta}{\cos\theta'} - 1\right)(1-\sec\theta)], \quad (17a)$$

$$b_{\phi\phi} = r\sin(\theta'-\theta)[1 + n(1-\cos\theta)(\cos\theta' - n\cos\theta)], \quad (17b)$$

$$b_{\theta\phi} = 0. \quad (17c)$$

Since $g_{\theta\phi} = 0 = b_{\theta\phi}$, the curves on the wave front surface θ = constant and ϕ = constant are along the principal directions. The principal curvatures of the refracted wave front surface, K_θ and K_ϕ, can be expressed by combining Eqs. (16) and (17) to give

$$K_\theta = \frac{b_{\theta\theta}}{g_{\theta\theta}} = \frac{n\cos\theta - \cos\theta'}{R[\cos^2\theta' + n(\cos\theta - 1)(n\cos\theta - \cos\theta')]}, \quad (18a)$$

$$K_\phi = \frac{b_{\phi\phi}}{g_{\phi\phi}} = \frac{n\cos\theta - \cos\theta'}{R[1 + n(1-\cos\theta)(n\cos\theta - \cos\theta')]}. \quad (18b)$$

Equations (18a) and (18b) give the principal radii of curvature of the refracted wave front as it passes through the exit pupil. For the axial incidence along the optical axis, $\theta = 0 = \theta'$, Eqs. (18a) and (18b) reduce to

$$K_\theta = K_\phi = \frac{n-1}{R}. \quad (19)$$

The values of K_θ and K_ϕ as a function of the normalized height (ρ_0/R) for the on-axis incidence on the plano-convex lens are presented in Fig. 5. The values of K_θ increase more rapidly than the corresponding values of K_ϕ for increasing values of normalized entrance pupil radius, which means that the image will be more spread out in the tangential direction than in the sagittal direction.

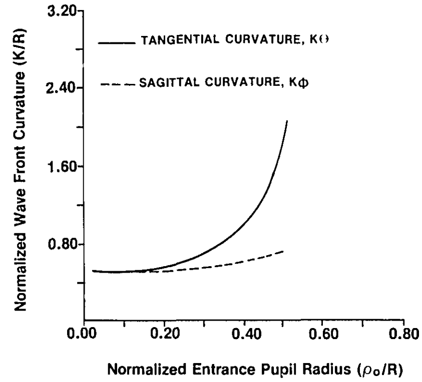

Fig. 5. Principal curvatures of the refracted wave front as a function of the normalized pupil radius for on-axis incidence on a plano-convex lens.

IV. Characteristics of Caustic Surfaces

The caustic surface is a double-sheeted 3-D surface in the image space which represents the loci of the sagittal and the tangential focal points of the optical systems.[16] The position vectors of the tangency points of the emerging ray with the caustic surface in the tangential and sagittal planes are given[15,16] by

$$\mathbf{X}_c = \mathbf{X}_m + r_c\hat{A}, \quad (20a)$$

$$\mathbf{X}'_c = \mathbf{X}_m + r'_c\hat{A}, \quad (20b)$$

where r_c and r'_c are the distances along the emerging ray measured from the last optical surface to the tangency points of that ray with the tangential and sagittal caustic surfaces, respectively. In Ref. 15, analytical expressions for r_c and r'_c have been derived by evaluating the loci of singularities in the flux density formula in image space.

In this study, an alternative approach will be given for evaluating r_c and r'_c, using the emergent wave front equation for on-axis incidence on a spherical reflector and a plano-convex lens. Since K_θ and K_ϕ are the principal curvatures of the wave front, r_c and r'_c can be expressed as

$$r_c = |\mathbf{X}_m - \mathbf{X}_c| = \delta + 1/K_\theta, \quad (21a)$$

$$r'_c = |\mathbf{X}_m - \mathbf{X}_c| = \delta + 1/K_\phi, \quad (21b)$$

where δ is equal to the distance along the ray measured from the reflector surface to the emerging wave front surface. From Eqs. (7) and (8), one can write for the spherical mirror

$$\delta = |\mathbf{X}_m - \mathbf{X}_w| = R(1-\cos\theta). \quad (22)$$

Combining Eqs. (11), (21), and (22) gives

$$r_c = (R/2)\cos\theta, \quad (23a)$$

$$r'_c = R/(2\cos\theta). \quad (23b)$$

Equations (23a) and (23b) are equivalent to those given in Ref. 15 obtained by an alternate approach.

Similarly, for on-axis incidence on the plano-convex lens, Eqs. (21a) and (21b) can be used to evaluate r_c and r_c' where δ is given by

$$\delta = nR(1 - \cos\theta). \tag{24}$$

Combining Eqs. (18), (21), and (24) gives

$$r_c = R\cos^2\theta'/(n\cos\theta - \cos\theta'), \tag{25a}$$

$$r_c' = R/(n\cos\theta - \cos\theta'). \tag{25b}$$

Equations (25a) and (25b) are equivalent to those given in Ref. 15 for the on-axis incidence on a plano-convex lens obtained by an alternate approach.

V. Wave Aberration Function for Spherical Mirror

In Sec. III, the wave front equation for a spherical reflector, Eq. (8), and a plano-convex lens, Eq. (15), have been used to derive expressions for the principal radii of curvature of the wave front, whose loci define the caustic surfaces of the system. In this section, the wave front equation for an off-axis plane wave reflected from a spherical mirror is derived and used to obtain a closed form expression for the wave aberration function for these systems.

Consider a collimated ray in xz plane making an angle α with the optical axis. Then a unit vector $\hat{A}_0$ along the incident ray is given by

$$\hat{A}_0 = -\sin\alpha\hat{\imath} + \cos\alpha\hat{k}. \tag{26}$$

Using the law of reflection, the unit vector $\hat{A}$ along the reflected ray is given by

$$\hat{A}(\theta,\phi) = -\sin(2\theta + \alpha)(\cos\phi\hat{\imath} + \sin\phi\hat{\jmath}) - \cos(2\theta + \alpha)\hat{k}. \tag{27}$$

Since the object point is at infinity, the incident wave front can be represented by a reference plane located at the origin or coordinate system, making an angle α with the entrance pupil (see Fig. 6).

For off-axis incidence on a spherical reflector in air, an equation for the reflected wave front $\mathbf{X}_w(\theta,\phi)$ is given by

$$\mathbf{X}_w(\theta,\phi) = \mathbf{X}_m(\theta,\phi) + (\psi_0 - r)\hat{A}(\theta,\phi), \tag{28}$$

where $(\psi_0 - r)$ is the optical path distance from the point of reflection $\mathbf{X}_m$ (θ,ϕ) to the reflected wave front and

$$\mathbf{X}_m(\theta,\phi) = R(\sin\theta\cos\theta\hat{\imath} + \sin\theta\sin\theta\hat{\jmath} + \cos\theta\hat{k}). \tag{29}$$

ψ_0 is the optical path length of the principal ray measured from the reference plane along the ray to the center of exit pupil E, and r is the optical path of an arbitrary ray measured along this ray from the reference plane to the incident point on the spherical reflector $\mathbf{X}_m$ (see Fig. 6). Then

$$\psi_0 - r = R[\cos\alpha - \cos(\alpha + \theta)]. \tag{30}$$

Combining Eqs. (29) and (30) with Eq. (28) gives

$$\begin{aligned}\mathbf{X}_w(\theta,\phi) = {} & R\{\sin\theta - [\cos\alpha - \cos(\alpha + \theta)]\sin(2\theta + \alpha)\} \\ & * (\cos\theta\hat{\imath} + \sin\phi\hat{\jmath}) \\ & + R\{\cos\theta - [\cos\alpha - \cos(\alpha + \theta)]\cos(2\theta + \alpha)\}\hat{k}. \end{aligned} \tag{31}$$

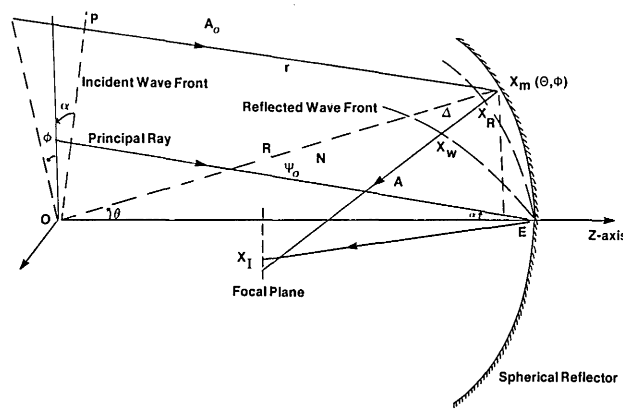

Fig. 6. Wave aberration function for off-axis incidence on a spherical reflector.

Equations (31) represent an exact expression for the reflected wave front surface as it passes through the exit pupil.

The conventional wave aberration function[12], Δ is defined as the distance along a real ray between an imaginary spherical wave front as it passes through the exit pupil. Referring to Fig. 6, an exact expression for the wave aberration function can be written as

$$\Delta(x_p,y_p;\alpha) = |\mathbf{X}_w(x_p,y_p;\alpha) - \mathbf{X}_R(x_p,y_p;\alpha)|, \tag{32}$$

where $\mathbf{X}_R$ is the position vector of a point on the reflected ray and the reference spherical wave front centered at the principal ray image point. Using the equation of a straight line along a ray connecting $\mathbf{X}_w$ and $\mathbf{X}_R$, Eq. (36) can be simplified as follows:

$$\Delta(x_p,y_p;\alpha) = (Z_w - Z_R)/A_z, \tag{33}$$

where A_Z is the z component of the unit vector $\hat{A}$ along the reflected ray. Z_w and Z_R are the z coordinates of the position vectors $\mathbf{X}_w$ and $\mathbf{X}_R$, respectively.

The coordinates (X_R,Y_R,Z_R) are related through the equation of a straight line connecting the points $\mathbf{X}_m$ and $\mathbf{X}_R$ (see Fig. 6) as follows:

$$\frac{X_R - R\sin\theta\cos\phi}{Z_R - R\cos\theta} = \frac{A_X}{A_Z} = \tan(2\theta + \alpha)\cos\phi; \tag{34a}$$

$$\frac{Y_R - R\sin\theta\sin\phi}{Z_R - R\cos\theta} = \frac{A_Y}{A_Z} = \tan(2\theta + \alpha)\sin\phi, \tag{34b}$$

where (A_X,A_Y,A_Z) are the direction cosines of the reflected ray given by Eq. (6). Since the coordinates of the center of the reference sphere $\mathbf{X}_I$ are $[-(R/2)\tan\alpha, 0, R/2]$, and its radius is $(R/2)\sec\alpha$ (see Fig. 6), the coordinates (X_R,Y_R,Z_R) are also related by the equation of the reference spherical wave front:

$$\left(X_R + \frac{R}{2}\tan\alpha\right)^2 + Y_R^2 + \left(Z_R - \frac{R}{2}\right)^2 = \left(\frac{R}{2}\sec\alpha\right)^2. \tag{35}$$

Solving Eqs. (34a) and (34b) and Eq. (35) for Z_R gives a quadratic equation

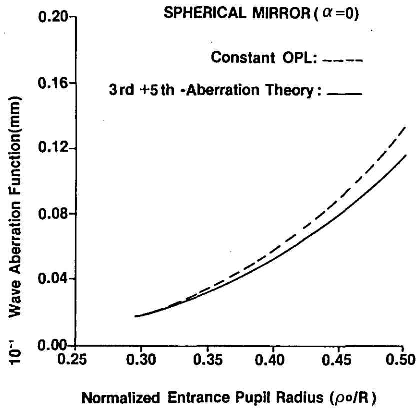

Fig. 7. Wave aberration function for on-axis incidence on a spherical reflector as a function of entrance pupil radius.

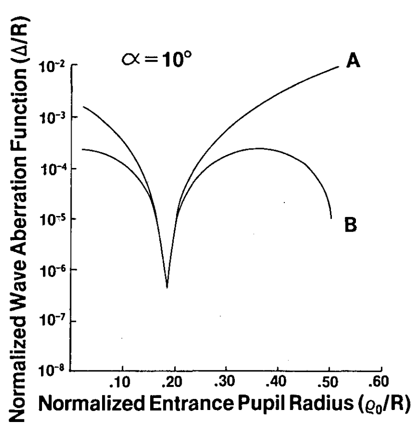

Fig. 8. Comparison of the normalized value of the wave aberration function, computed by the conventional definition (a) and by the results of third-order aberration theory (b) as a function of the normalized entrance pupil radius for off-axis incidence on a spherical reflector.

$$
\begin{aligned}
&Z_R^2 + R[\sin\theta \sin(4\theta + 2\alpha) - 2 \cos\theta \sin^2(2\theta + \alpha) \\
&\quad + \frac{\tan\alpha}{2} \sin(4\theta + 2\alpha) \\
&\quad - \cos^2(2\theta + \alpha)]Z_R + R^2[\cos(4\theta + 2\alpha) \\
&\quad \times (\sin\theta \cos\phi \tan\alpha + \sin^2\theta) \\
&\quad + (1 - \sin 2\theta) \sin^2(2\theta + \alpha)]. \qquad (36)
\end{aligned}
$$

Equation (36) is solved for Z_R by using the quadratic formula, where the valid solution should satisfy the condition $Z_R = 0$ for α and $\theta = 0$. The result is

$$Z_R = R(-B + \sqrt{B^2 - L^2})/2, \qquad (37)$$

where

$$
\begin{aligned}
B &= \sin\theta \sin(4\theta + 2\alpha) - 2\cos\theta \sin^2(2\theta + a) \\
&\quad + \frac{\tan\alpha}{2} \sin(4\theta + 2\alpha) \cos\phi - \cos^2(2\theta + \alpha), \\
L &= 4 \sin(\theta + \alpha)[\sin(\theta + \alpha) - \tan\alpha \cos^2(2\theta + a) \cos\phi].
\end{aligned}
$$

Combining Eq. (33) with Eqs. (27), (31), and (37) gives the wave aberration function for collimated off-axis rays reflected from a spherical mirror:

$$
\begin{aligned}
\Delta = &-\frac{R}{\cos(2\theta + \alpha)} \{\cos\theta - [\cos\alpha - \cos(\alpha + \theta)] \cos(2\theta + \alpha) \\
&+ (B - \sqrt{B^2 - L^2})/2\}. \qquad (38)
\end{aligned}
$$

Values for Δ computed from Eq. (38) have been compared with the values of this function given by the third and fifth-order aberration theory[17] in Figs. 7 and 8. Referring to Figs. 7 and 8, the corresponding values of (Δ/R) computed by Eq. (38) and the results of the third- and fifth-order aberration theory have been compared as a function of the normalized entrance pupil radius ($\rho_0/R = \sin\theta$) for the field angle of 0 and 10°. Both values for Δ/R converge for paraxial incidence on the spherical reflector.

IV. Conclusion

The generalized wave front equation has been evaluated for an on-axis plane wave reflected from a spherical mirror and a plano-convex lens and for an off-axis plane wave reflected from a spherical mirror. From the wave front equation of these systems, the principal wave front curvatures, which locate the caustic surfaces of the system, and the wave aberration function have been evaluated in closed form. The results have been compared to third- and fifth-order aberration theory, which quantify the limits of applicability of the approximate theories. Extension of these techniques for evaluating the aberration function of more general optical systems is under investigation.

To apply this technique to evaluation the wave aberration function of a more general optical system, one must be able to perform an analytical ray trace of the system. In principle, an analytical ray trace can be done for plane or spherical wave light reflected or refracted from a multi-interface spherically shaped optical system, although the algebraic details become overwhelming unless one uses a symbolic manipulation program on a computer such as MACSYMA.[24]

References

1. M. Born and E. Wolf *Principles of Optics* (Pergamon, New York, 1959), pp. 108–29.
2. J. L. Synge, and W. Corway, *The Mathematical Papers of Hamilton* (Cambridge U. P., London, 1931).
3. V. A. Fock, *Electromagnetic Diffraction and Propagation Problem* (Pergamon, New York, 1960), p. 160.
4. O. N. Stavroudis, and R. C. Fronczek, "Caustic Surfaces and the Structure of the Geometrical Optics," J. Opt. Soc. Am. **66,** 795 (1976).
5. O. N. Stavroudis, "Tracing Wavefronts: Can it be Done?," Proc. Soc. Photo-Opt. Instrum. Eng. **766,** 18 (1987).
6. J. A. Kneisly, "Local Curvature of Wave Fronts in an Optical System," J. Opt. Soc. Am. **54,** 229 (1964).
7. J. M. Rebordao, and M. Grosmann, "Refraction on Spherical Surfaces. I: an Exact Algebraic Approach," J. Opt. Soc. Am. A **1,** 51 (1984).
8. L. Seidel, "On Dioptics on the Development of Third Order Coefficients," Astron. Nachr. **43,** 289 (1956).
9. H. A. Buchdahl, *Optical Aberration Coefficients* (Dover, New York, 1968), p. 35.

10. P. J. Sands, "Off-Axis Aberration Coefficients," Thesis, Australian National University, Australia (1967).
11. W. T. Welford, "A New Total Aberration Formula," Opt. Acta **19,** No. 9, 719 (1972).
12. H. H. Hopkins, *Wave Theory of Aberrations* (Oxford U.P., London, 1950), Chap. 1.
13. W. T. Welford, *Aberration of the Symmetrical Optical System* (Academic, New York, 1974), pp. 4–45.
14. E. Kreyszig, *Introduction to Differential Geometry and Riemannian* (U. Toronto Press, Toronto, Ont., 1968), pp. 57–99.
15. D. G. Burkhard, and D. L. Shealy, "Formula for the Density of Tangent Rays over a Caustic Surface," Appl. Opt. 21, 3299 (1982).
16. O. N. Stavroudis, *The Optics of Rays, Wave Front and Caustics* (Academic, New York, 1972), p. 157.
17. B. R. Nijboer, "Title," Physica **10,** 679 (1943).
18. E. L. O'Neil, *Introduction to Statistical Optics* (Addison-Wesley, Reading, MA 1963), Chap. 4.
19. D. L. Shealy and D. G. Burkhard, "Analytical Illuminance Calculation in a Multi-Surface Optical System," Opt. Acta **22,** 485 (1975).
20. W. J. Smith, *Modern Optical Engineering* (McGraw-Hill, New York, 1966).
21. M. Schwartz, S. Green, and W. A. Rutledge, *Vector Analysis* (Harper & Row, New York, 1969).
22. F. A. Jenkins and H. E. White, *Fundamentals of Optics* (McGraw-Hill, New York, 1957), p. 173.
23. M. Herzberger, *Modern Geometrical Optics* (Wiley-Interscience, New York, 1958), pp. 299–379.
24. SYMBOLIC, Inc., Eleven Cambridge Center, Cambridge, MA 02142.

NASA *continued from page 504*

This work was done by Mysore Lakshminarayana of Caltech for NASA's Jet Propulsion Laboratory. Refer to NPO-16836.

Frequency-modulated to digital converter

An inexpensive circuit converts a frequency-modulated (FM) signal into a digital signal. The circuit consists of a zero-crossing detector and a series of monostable multivibrators and *D*-type flip-flops.

The zero crossings of the FM input are detected and converted to pulses at a voltage compatible with transistor/transistor logic. These pulses are fed to the monostable multivibrators and flip-flops. The positive-going edge of a pulse changes the output of a multivibrator from its normal 1 to a 0. The duration T_i of the 0 output of each multivibrator equals that of its predecessor in the chain minus a small decrement of time: $T_{i+1} = T_i - \Delta T$. In a chain of N monostable/D flip-flop pairs, T_1 is half the reciprocal of the lowest frequency to be detected, and T_N is half the reciprocal of the highest frequency to be detected.

When a multivibrator returns to its logic 1 state, it clocks the zero-crossing data from the input to the output of its flip-flop. If the duration of a zero-crossing pulse is shorter than the duration T_k of the logic 0 state of the kth multivibrator, a logic 0 will be clocked out of flip-flop D_k. If the zero-crossing pulse is longer than T_k, a logic 1 is clocked out of flip-flop D_k. In the example of Fig. 7, the zero-crossing pulse is shorter than T_2 but longer than T_3, signifying a frequency somewhere between $1/(2T_2)$ and $1/(2T_3)$.

The pattern of ones and zeros on the flip-flop outputs thus represents the input frequency. As the frequency increases, the zero-crossing pulses grow shorter and the pattern changes. The more multivibrators there are, the more patterns there will be and the more precisely the input frequency can be resolved.

The circuit might also be used to control a filter. As frequency changes are detected, the binary output could be fed to an attenuator or amplifier to reduce or increase the gain; unwanted frequencies in a signal would thus be suppressed.

The multivibrator circuit offers important advantages over other ways of converting FM signals to binary signals. Compared with phase-locked loops and constant-energy, pulse averaging circuits, it has fewer components and responds more quickly.

This work was done by Michael Moniuszko of Ames Research Center. Inquiries concerning rights for the commercial use of this invention should be addressed to the Patent Counsel, NASA Ames Research Center, M.C. 200–11, Moffett Field, CA 94035. Refer to ARC-11172.

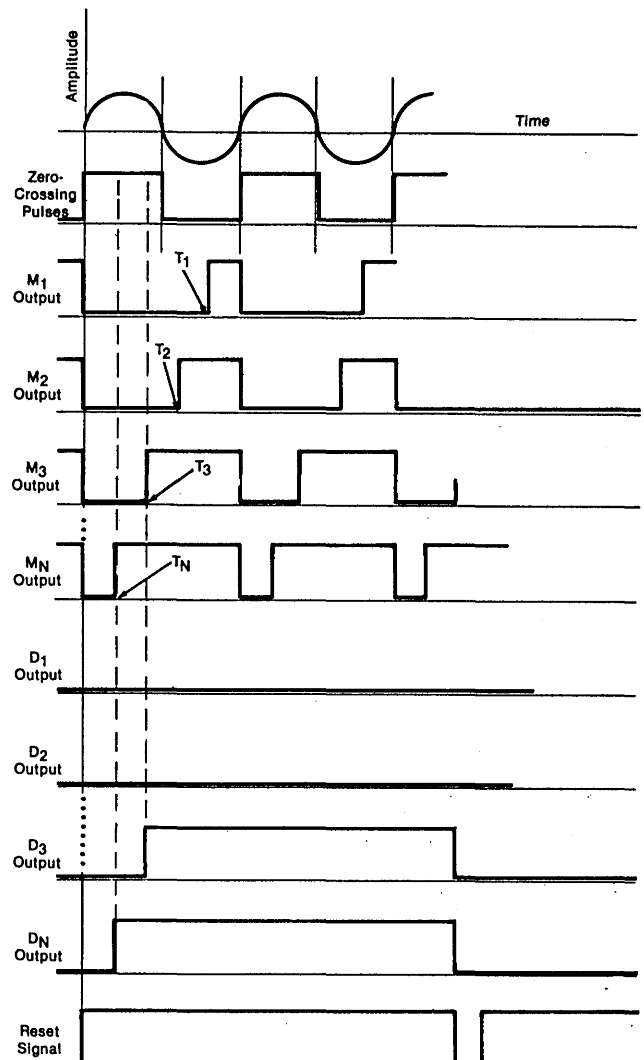

Fig. 7. Timing relationships between the zero-crossing pulses and the logical-zero output intervals of the monostable multivibrators determine the pattern of ones and zeros at the outputs. Here, the frequency lies between $f_2 = 1/(2T_2)$ and $f_3 = 1(2T_3)$.